Separation Science and Technology
Publication details, including instructions for authors and subscription information:
http://www.informaworld.com/smpp/title~content=t713708471

Parameter Estimation of Cyclobutane Pyrimidine Dimers and Monomers of Uracil and Thymine in Reversed-Phase High Performance Liquid Chromatography

Kyung Ho Row[a]; Jung Ik Raw[b]
[a] SEPARATION PROCESS LABORATORY DIVISION OF CHEMICAL ENGINEERING KOREA INSTITUTE OF SCIENCE AND TECHNOLOGY, SEOUL, KOREA [b] DEPARTMENT OF TEXTILE ENGINEERING, COLLEGE OF ENGINEERING INHA UNIVERSITY, INCHEON, KOREA

To cite this Article Row, Kyung Ho and Raw, Jung Ik(1991) 'Parameter Estimation of Cyclobutane Pyrimidine Dimers and Monomers of Uracil and Thymine in Reversed-Phase High Performance Liquid Chromatography', Separation Science and Technology, 26: 1, 15 — 23
To link to this Article: DOI: 10.1080/01496399108050453
URL: http://dx.doi.org/10.1080/01496399108050453

SEPARATION SCIENCE AND TECHNOLOGY, 26(1), pp. 15–23, 1991

Parameter Estimation of Cyclobutane Pyrimidine Dimers and Monomers of Uracil and Thymine in Reversed-Phase High Performance Liquid Chromatography

KYUNG HO ROW

SEPARATION PROCESS LABORATORY
DIVISION OF CHEMICAL ENGINEERING
KOREA INSTITUTE OF SCIENCE AND TECHNOLOGY
P.O. BOX 131, CHEONGRYANG, SEOUL, KOREA

JUNG IK RAW

DEPARTMENT OF TEXTILE ENGINEERING
COLLEGE OF ENGINEERING
INHA UNIVERSITY
253, YONGHYEON-DONG, NAM-KU, INCHEON, KOREA

Abstract

Cyclobutane pyrimidine dimers and monomers of uracil and thymine were separated on a C18 reversed-phase high performance liquid chromatographic column. Rate and equilibrium constants were determined by analyzing the moments of the elution curves. Based on the parameters estimated, the comparison between the experimental and calculated values was good. The experimental results showed that optimum resolutions were obtained at 1.0 mL/min of flow rate eluant.

1. INTRODUCTION

Exposure of DNA to near- or far-UV radiation results in the formation of lesions, of which the pyrimidine dimers are the most abundant (*1*, *2*). The cyclobutane pyrimidine dimers are thought to be the major DNA photoproduct lesion. These lesions provide a model for the study of molecular repair processes in damaged DNA and therefore constitute an important class of compounds. Because of the low concentration of the dimers and the small quantity of material that is usually available for analysis, sensitive methods are required for accurate determination.

In the present work, the cyclobutane pyrimidine dimers and monomers of uracil and thymine are considered for reversed-phase high performance

chromatographic separation. Model equations were established based on the linearity of the equilibrium isotherm (*3*). The first two moments are derived from the solution in the Laplace domain, but they are a function of eluant flow rate.

2. EXPERIMENTS

The samples were analyzed on a Waters liquid chromatographic system equipped with a Model 600E multisolvent delivery system, a Model U6K injector, and a Model 490 programmable multiwavelength detector. Data acquisition was performed by a Maxima 820 chromatography workstation. The LC effluent was simultaneously monitored at two different wavelengths corresponding to the absorption maxima for the monomers (254 nm) and dimers (210 nm). With the C18 Adsorbosphere HS column (Alltech Associates), chromatographic elution curves were obtained at atmospheric pressure and room temperature. The mobile phase was water/2% methanol. In this work, five solutes, the cyclobutane pyrimidine dimers, thymine–thymine dimer (T-T), uracil–uracil dimer (U-U), thymine–uracil dimer (T-U), plus the monomers, thymine (T) and uracil (U), are considered for chromatographic separation. The dimers were prepared by Dr. Ho at the Oak Ridge National Laboratory. HPLC-grade water was used as the solvent in these experiments. The dimensions of the column were 25 cm long and 0.46 cm i.d., and the column was packed with 7 μm particles. The flow rates of the eluant ranged from 0.5 to 1.5 mL/min at ambient temperatures.

For each operation a 10-μL sample solution at a concentration of 25 ng/μL was injected to provide data for calculating the rate and equilibrium coefficient. To verify the linear range of the samples, five different sample sizes of from 0.1 to 20.0 μg were injected.

3. BASIC EQUATIONS

The kinetic mathematical model is used to predict the concentration profile of pyrimidine photoproduct dimers and monomers and to assist in optimization of cut points for HPLC fraction collection. This will aid in the isolation of photo-induced dimers for quantitative analysis. The equations in the kinetic model present the local average solute concentration in the column and in the intraparticle voids in terms of various transport parameters such as axial dispersion coefficient, interparticle coefficient, intraparticle coefficient, and effective intraparticle diffusion coefficient (*3*, *4*).

$$\frac{\partial c}{\partial t} + u\frac{\partial c}{\partial z} = \frac{E\partial^2 c}{\partial z^2} - \frac{3}{r_p}\frac{(1-\epsilon)\epsilon_p}{\epsilon} D_e \frac{\partial q}{\partial r}\bigg|_{r=r_p} \tag{1}$$

$$\frac{\partial q}{\partial t} = D_e \frac{1}{r^2}\frac{\partial}{\partial r}\left(r^2 \frac{\partial q}{\partial r}\right) - \frac{\partial n}{\partial t} \tag{2}$$

$$\partial n/\partial t = k_a(q - n/K_e) \tag{3}$$

The initial and boundary conditions are:

$$c = q = n = 0 \qquad (\text{for } t \le 0,\ z > 0) \tag{4}$$

$$c = \delta(t) \qquad (\text{for } t > 0,\ z = 0) \tag{5}$$

$$c = \text{finite} \qquad (\text{for } t > 0,\ z \to \infty) \tag{6}$$

$$\partial q/\partial r = 0 \qquad (\text{for } t > 0,\ x = 0) \tag{7}$$

$$D_e \frac{\partial q}{\partial r} = k_f (c - q) \qquad (\text{for } t > 0,\ r = r_p) \tag{8}$$

It is assumed that the adsorption effect is dominant with a linear equilibrium isotherm. The solution of Eq. (1) to Eq. (8) in the Laplace domain is

$$\overline{C}(s,L) = \exp\left(\frac{Lu}{2E} - L\left[\left(\frac{u}{2E}\right)^2 + \frac{\gamma}{E}\right]^{1/2}\right) \tag{9}$$

at the bed exit, $z = L$, where

$$\gamma = s + \frac{3k_f}{r_p}\gamma_3\left(1 - \frac{1}{1 - \gamma_1 + \gamma_1\gamma_2 \coth \gamma_2}\right) \tag{10}$$

$$\gamma_1 = \frac{D_e}{r_p k_f} \tag{11}$$

$$\gamma_2 = r_p\sqrt{\frac{s}{D_e}\left(1 + \frac{K_e k_a}{K_e s + k_a}\right)} \tag{12}$$

$$\gamma_3 = \frac{(1 - \epsilon)\epsilon_p}{\epsilon} \tag{13}$$

The first two moments can be obtained by applying the final value theorem of the Laplace transform,

$$m_1' = \frac{L}{u}(1 + \gamma_3(1 + K_e)) \tag{14}$$

$$m_2 = \frac{2EL}{u^3}[1 + \gamma_3(1 + K_e)]^2 + \frac{2L\gamma_3}{u}\left[\frac{K_e^2}{k_a} + \frac{r_p(1 + K_e)^2}{3}\left(\frac{1}{k_f} + \frac{r_p}{5D_e}\right)\right] \tag{15}$$

where m_1' indicates the first noncentral moment and m_2 is the second central moment, i.e., mean and variance.

In order to predict the concentration curves, the transport parameters should be estimated. In this work the moment method is used to evaluate rate and equilibrium constants, and the first and second moments are sufficient to establish resolution criteria.

4. RESULTS AND DISCUSSION

A necessary condition for the chromatographic model employed here is the linearity of the equilibrium isotherm. This is shown in Fig. 1, which

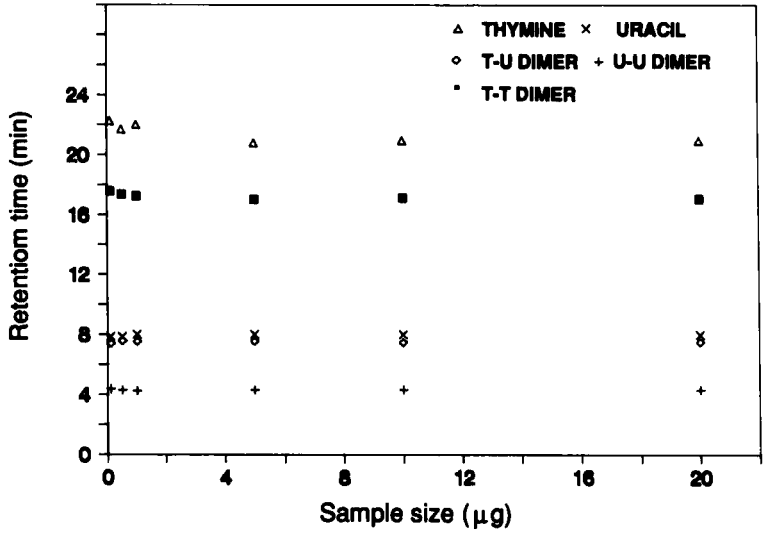

FIG. 1. Effect of sample size on retention time (eluant flow rate = 1.0 mL/min, amount of injection = 0.5 μg).

indicates that the retention times were independent of the concentration in the injected pulse. The elution order is uracil dimer, uracil–thymine dimer, uracil, thymine dimer, and thymine. The simple linear regression method was adopted to calculate the partition coefficients of the five components from Eq. (14). From the equation, it follows that

$$\frac{m_1'}{L} = \frac{1}{u}(1 + \gamma_3(1 + K_e)) \tag{16}$$

A plot of m_1'/L vs $1/u$ should be a straight line through the origin, and the slope gives $(1 + \gamma_3(1 + K_e))$, as shown in Fig. 2. The orders of the magnitude of the slopes are identical to the elution orders of the five components. These are important results for developing linear mathematical models within the concentration range examined in this experiment.

Each of the response curves was fit to the transient material balance with the adjustable parameters to find the variance. The void fraction of the bed (ϵ) and the internal porosity of the particle (ϵ_p) were assumed to be 0.4 and 0.5, respectively. Unlike axial dispersion in gaseous systems (5), axial dispersion in liquid systems is directly proportional to the eluant flow rate because of low diffusivity. Therefore, the equation $E = \eta r_p u$

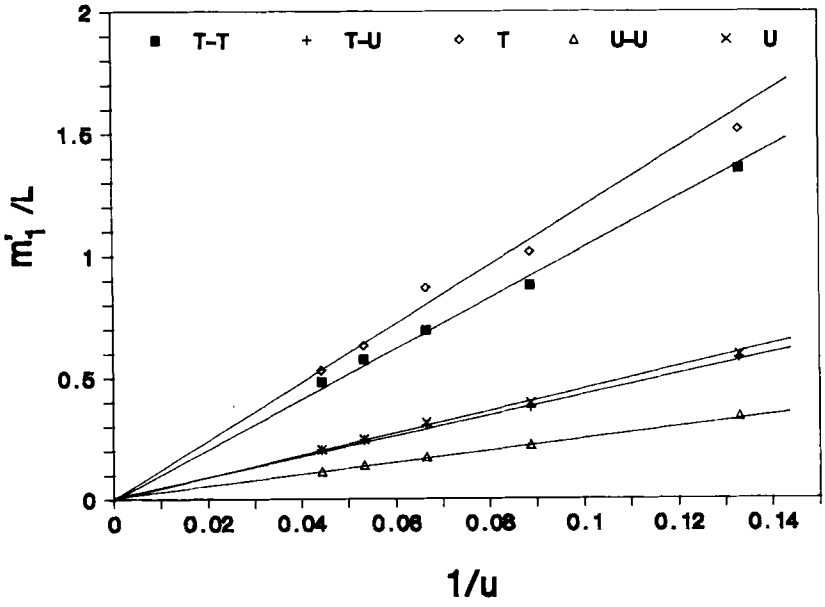

FIG. 2. Dependence of m_1'/L on $1/u$ (same experimental condition as in Fig. 1).

can be used. The dependence of film diffusion on flow rate can be incorporated by the following semiempirical correlation of Foo and Rice (*6*):

$$2r_p k_f / D_M = 2 + 1.45\mathrm{Re}^{0.5}\mathrm{Sc}^{0.3}$$

The molecular diffusivity, D_M, was calculated from the Wilke-Chang equation by using the molar volume of the diffusing solute (*7*). The diffusivity of the samples was almost the same as 0.00057 cm^2/min because it was mainly affected by the solvent. The interparticle mass transfer coefficients, k_f, with the superficial flow rates were 19.85, 23.95, 27.40, 30.44, and 33.19 cm/min for 0.50, 0.75, 1.00, 1.25, and 1.50 mL/min, respectively. Therefore, Eq. (15) can be used to evaluate the rate constants k_a, E, and D_e. They cannot be determined by simple linear regression used in the partition coefficients because of the nonlinearity of the expression with respect to eluant velocity. Consequently, the nonlinear optimization method was used. Table 1 lists the resulting values.

The rate constants determined can be used to predict the elution curves by transforming Eqs. (9) to (13) into the real time domain. Among many approximation techniques, the equations were inverted numerically from the curve-fitting procedure by Dang and Gibilaro (*8*). The agreement between the experimental data and the predicted elution curve is fairly good (see Fig. 3).

Figure 4 shows the effect of the flow rate of the eluant on experimental resolution, which is defined by

$$R_{ij} = 2(t_{Rj} - t_{Ri})/(w_j + w_i) \tag{17}$$

where R_{ij} = resolution between components i and j. The maximum resolution under our experimental conditions is in the range of 1 mL/min. It was found from the simulation results that about 75 cm of column length is required to resolve T-U and U at an eluant flow rate of 1 mL/min.

TABLE 1
Partition and Rate Constants of Cyclobutane Pyrimidine Dimers and Monomers of Uracil and Thymine on RP-HPLC Column

	U-U	T-U	U	T-T	T
K_c	1.1	3.7	4.0	11.7	13.3
η	19.6	36.9	74.2	19.3	39.4
k_a (1/min)	66.7	573.1	220.3	1194.7	1965.5
D_e (cm^2/min)	1.0	1.4	1.1	5.3	7.0

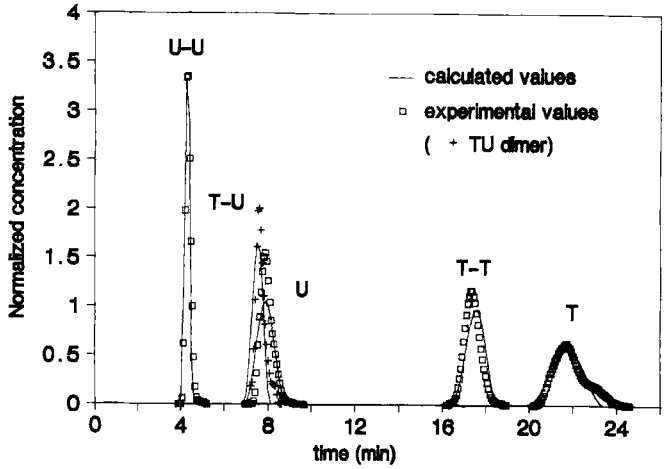

FIG. 3. Comparison of experimental data with the predicted elution curve (same experimental condition as in Fig. 1).

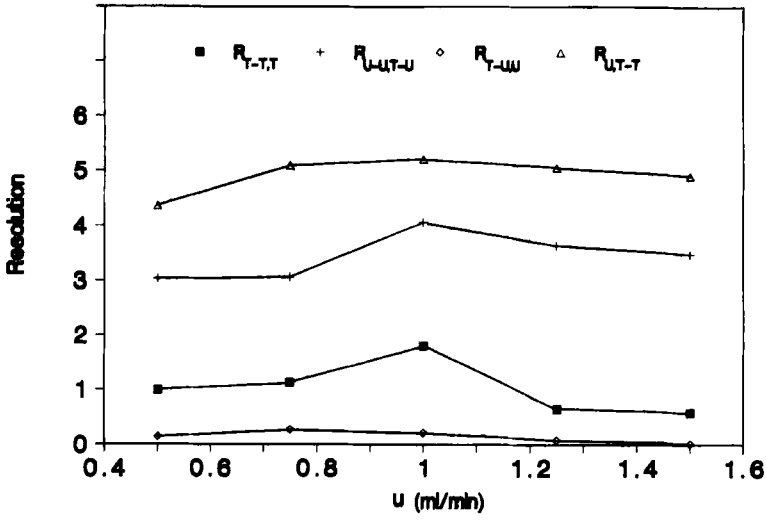

FIG. 4. Effect of eluant flow rate on the experimental resolution (amount of injection = 0.5 μg).

NOTATION

c	concentration of solute in the mobile phase (mol/m^3)
c_0	inlet concentration of solute (mol/m^3)
$C(s)$	Laplace transform of $c(t)$
D_e	diffusion coefficient in the pore spacing (m^2/s)
D_M	molecular diffusivity (m^2/s)
E	axial dispersion coefficient (m^2/s)
k_a	adsorption rate constant (1/s)
k_f	interparticle mass transfer coefficient (m/s)
K_e	adsorption rate constant
L	column length in the partition section and the desorption section (m)
n	concentration of solute adsorbed on the pore surface (mol/m^3)
q	concentration of solute in the pore spacing (mol/m^3)
r	radial distance (m)
r_p	radius of porous particle (m)
Re	Reynolds number
R_{ij}	resolution between i and j components
s	variable of Laplace transform
Sc	Schmidt number
t	time
t_{Ri}	retention time of i component
u	interstitial velocity of carrier gas or desorbent (m/s)
w_i	peak width of i components
x	distance perpendicular to surface of porous particle (m)
z	axial distance (m)

Greek Letters

γ, γ_1, γ_2, γ_3	values defined by Eqs. (10) to (13)
ϵ	void fraction of chromatographic column
ϵ_p	intraparticle porosity
η	coefficient for axial dispersion

Acknowledgment

The experimental work was performed at Oak Ridge National Laboratory, Tennessee.

REFERENCES

1. J. Cadet, N. E. Gentner, and M. C. Paterson, *J. Chromatogr., 280,* 99 (1983).
2. J. D. Love and E. C. Friedberg, *Ibid., 240,* 475 (1982).

3. P. Schneider and J. M. Smith, *AIChE J.*, *14*, 762 (1968).
4. Y. S. Ghim and H. N. Chang, *Ind. Eng. Chem., Fundam.*, *21*, 369 (1982).
5. K. H. Row and W. K. Lee, *J. Chem. Eng., Jpn.*, *19*, 173 (1986).
6. S. C. Foo and R. G. Rice, *AIChE J.*, *21*, 1149 (1975).
7. C. R. Wilke and P. Chang, *Ibid.*, *1*, 264 (1955).
8. N. D. P. Dang and L. G. Gibilaro, *Chem. Eng., J.*, *8*, 157 (1974).

Received by editor February 9, 1990